LA-UR-93-3469

Los Alamos National Laboratory is operated by the University of California for the United States Department of Energy under contract W-7405-ENG-36

TITLE: **A VIRTUAL PROTOTYPE FOR AN EXPLOSIVES DETECTION SYSTEM**

AUTHOR(S): Tom Seed, Barry Berman, and John D. Zahrt

SUBMITTED TO: Substance Identification Technology
Innsbruck, Austria
October 4-8, 1993

DISCLAIMER

Los Alamos

Los Alamos National Laboratory
Los Alamos New Mexico 87545

A VIRTUAL PROTOTYPE FOR AN EXPLOSIVES DETECTION SYSTEM

Tom Seed, Barry L. Berman*, and John D. Zahrt
Los Alamos National Laboratory, Los Alamos, NM 87545

***Permanent address: Dept. of Physics, The George Washington University, Washington, D.C. 20052**

I. INTRODUCTION

The development of the resonance-absorption based explosives detection system (EDS), as initially planned, involved the parallel development of a high-current proton accelerator (with a long development time) and the other detection subsystems. The design approach for the latter was to develop a capability for computer modeling the essential processes of each subsystem, benchmark these models by experiment, and link the models, i.e., creating a virtual prototype, to explore the effect of subsystem design changes on the EDS system performance. Additionally, when the EDS prototype system was completed, the linked models would be used to investigate further trade-offs in defining an airport system. Most of the necessary subsystem modeling was completed and used in subsystem design. Linking of all of the subsystems was accomplished to some degree or another.

There are many physical and mathematical processes that take place between the acceleration of the proton beam and the final display of the reconstructed image. Figure 1 summarizes these processes and indicates which code was used to model each particular process.

Section II reports on the modeling of the proton beam incident on a ^{11}C target. The gamma-ray output is the desired output from this phase of modeling. Section III describes the tools used to investigate the transport of the gamma-rays through computer simulated phantoms (suitcases). Two different codes were used in this investigation: a Monte Carlo photon transport code and a ray tracing code. One benchmark between these codes was accomplished. Section IV is concerned with the model calculations performed on single detectors. The calculations again were performed with a Monte Carlo transport code. The reconstruction code, used throughout in the simulations and as the workhorse in the analysis of the real experiments, is described in Section V. The graphics visualization and alarm procedure are discussed in Section VI. We conclude, in Section VII, with our assessment of the simulation/virtual prototyping of the real experiment.

II. MODELING OF THE PROTON BEAM AND ITS INTERACTION WITH THE TARGET

Modeling of the proton transport through the ^{11}C target and photon production from the $^{11}C\,(p,\gamma)$ reaction were done with LAHET (Los Alamos High Energy Transport), a Monte Carlo code. Several modifications to this code were necessary before we could use it for our applications. These included: i) including the ^{11}C cross sections for resonant and nonresonant proton interactions, ii) defining an arbitrary collision length which is a minimum at the proton resonance with ^{11}C, iii) sampling the photon emission angle and consequently the photon energy, and iv) recording the kinetic parameters of each photon to a file for use as input to MCNP.

For thick target yield calculations, MCNP was able to compute values in accordance with experimental values.

Figure 2 shows the results from allowing a 1.747 MeV beam of protons to interact with a ^{11}C target. The energy/angle dependence was consistent with theory.

III. GAMMA-RAY TRANSPORT IN SUITCASES

A. The Monte Carlo Method: The freely distributed code MCNP was used initially to model the transport of gamma rays through suitcases. This then provided the (count) data to be used in reconstruction. Originally MCNP lacked the necessary ^{14}N cross sections for the nuclear resonance-absorption process. These were added to the libraries, so that now MCNP has all of the presently recognized important physics built into it. It thus provides the most powerful and accurate way of modeling real experimental data. The power of building rather arbitrary shapes in the phantoms also is unsurpassed. However, the time required to obtain 5% data (a nominal 400 counts in each detector) for an entire model suitcase is nearly 24 hours on a CRAY (time shared).

B. The Ray Tracing Method: As modeling was proceeding with MCNP, a ray tracing code was developed that would create parallel, fan, or cone beam data for incorporation into the reconstruction code (see below). Promise for the ray tracing code came from MCNP itself when it demonstrated that scattering influenced only about one percent of the signal received by a detector. Indeed, ray tracing data and MCNP data (for the same phantom) gave nearly the same reconstruction when the ray trace cross section was adjusted slightly, as demonstrated in Figures 3 and 4. Here we had to use a 6 MeV cross section of 0.03 cm^{-1}, instead of the value 0.022 which we had been using.

The advantage of the ray tracing lies in its speed of execution: only minutes for a complete data set from a suitcase 10's of shees thick. Of course, not all of the physics is included in the ray tracing code. However, these subtleties appear to be lost in the coarseness of our data (few detectors, few views, and few counts).

IV. GAMMA-RAY DETECTION AND TRANSPORT IN DETECTORS

Detector modeling addressed several independent issues and took advantage of three different codes. MCNP was used to model several different aspects of the overall system. Figure 5 shows a MCNP simulation of a BGO detector with a multiple energy gamma-ray source from a composite ^{11}C and ^{19}F target. The escape peaks are readily seen in the spectra. MCNP also was used to compare the efficiency and resolution (the response functions) of BGO and NaI(Tl) detectors. The higher efficiency of a BGO detector, for a given size, was readily apparent.

Lead and tungsten collimators were modeled, with and without scattering from the slit. Little difference between the two collimator materials was seen, and slit scattering was shown to be unimportant.

Perhaps the most important question concerned what angles of emission from the target should be allowed to impinge on the detectors to provide the best detector resolution and statistics. Multiple runs demonstrated that an angular width of 0.75 degree was optimal. Smaller slit widths did not provide the necessary counting statistics, whereas larger widths degraded the resolution by introducing increased noise.

GUIDE7, a CERN code, was used to model the the transport of light through the detector to the photomultipher tube. Some effort was expended in getting GUIDE7 to accept a MCNP output. Then GUIDE7 calculations showed that with black front and side faces on the detector gave 37% efficiency while mirrored faces provided 95% efficiency. Finally, the most important result from GUIDE7 calculations has been to optimize size, shape and material of detectors and light guides. The optimal shape for the light guides is tapered sharply; the optimum material is also BGO.

EGS (Electron Gamma Shower), a SLAC code, contained the most explicit formulation of the electron and gamma ray interactions. It was used successfully in modeling the response of different sized BGO detectors.

V. RECONSTRUCTION BY THE METHOD OF CORMACK

In 1963 and 1964 A. M. Cormack published two seminal papers on the representation of a function by its line integrals [1,2] for which he was subsequently awarded the Nobel Prize. We began with his work and were able to generalize his method from parallel beam tomography to fan beam tomography (see the forthcoming paper by Faber, Joubert, Kust, Wing and Zaurt [3]). The essence of this method involves Fourier transforming the data in angle space (the angle of the projection), followed by a singular value decomposition solve for the Fourier coefficients of the solution. These are then back Fourier transformed (in angle space) to give the density (in units of cm-1). This was done for both the 6MeV and 7MeV data combined and for the 9MeV data. The individual tomograms were then subtracted to give the "nitrogram." That is,

$$a_{i,k}^{l,j} = \ln N_{i,k}^{l,j}/N_{i,k}^{0,j} \rightarrow (\rho\sigma_c)_{i,k} \tag{V.1}$$

$$a_{i,k}^{l',j} = \ln N_{i,k}^{l',j}/N_{i,k}^{0,j} \rightarrow (\rho\sigma_c + \rho f_N \sigma_n)_{i,k} \tag{V.2}$$

where i refers to the i th detector, j to the jth projection and/or to the jth polar angle, k is the slice index, and l' is the l'th polar radial discretization. The appropriate subtraction of (V.1) from (V.2) leaves the nitrogram, $(\rho f_N \sigma_n)_{i,k}$.

Figure 6 shows a slice of a three-dimensional reconstruction from computer simulated cone beam 6 MeV data.

Figure 7 shows the reconstruction of cobalt 60 gamma-ray data using 16 detectors and 32 views. The phantom was a hollow cylinder of 5 mm wall thickness.

Figure 8 shows the reconstruction of the 6 MeV data from real data [from $^{11}C(p,\gamma_0)$] gamma rays with 16 detectors and 32 views.

Given the geometry of our system, radius of the turntable of 55 cm and distance from source to turntable center of 94 cm, the two dimensional Cormack algorithm works quite well. Some artifacts are noticeable on the outer portions of the turntable and horizontal sheets sometimes move through two slices, however these artifacts are easily recognized.

VI. GRAPHICS AND ALARMS

KHOROS, a freely distributed image analysis, data analysis and 2D/3D graphics software environment was used throughout this project. (It is distributed by the University of New Mexico.) We have used KHOROS to look directly at the absorbence data, to estimate the noise level of the data, and to view the tomographic reconstructions.

Originally the alarm system was to be an integral part of the KHOROS platform. However the automated cesium source (used to define shapes of nitrogenous materials) did not work on real experiments as it did on computer simulations. Thus various alarm routines could, likewise, not be automated.

All of the tomography graphics, in this and accompanying papers were done with KHOROS.

VII. CONCLUSIONS

The complete virtual prototyping of the entire system eventually became victim to budgetary constraints. The technical issues prompted by the interfacing of all of the codes, each developed in isolation, had been overcome. A few model calculations provided good benchmarking against experimental data. However, certain key issues have not yet been modeled. Nevertheless, subsystem modeling was still very useful in guiding target design, detector design, and count requirements versus image resolution.

It does seem apparent, given our experience in this project, that the entire system can be modeled and linked together to provide computer experiments and optimizations, thus providing a low cost alternative to excessive laboratory measurements. Of course, the results of such simulations eventually need to be checked against experimental results.

VIII. ACKNOWLEDGEMENTS

We would like to thank the Federal Aviation Administration (USA) for support in performing this work under DTFA03-83-A-00321.

We would like to thank Trae Chancellor, Kristy Matthews, and Becky Caress for their contributions to the virtual prototyping not mentioned in this paper. Special thanks go to Robert Little for his help in getting the ^{14}N nuclear resonant cross section into the MCNP libraries and to Richard Prael for his help with LAHET. Jim White and Pat Kelly graciously provided support and software for KHOROS.

IX. References

[1] Cormack, A. M., *J. Appl. Phys.* **34**, 2722-2727 (1963).

[2] Cormack, A. M., *J. Appl. Phys.* **35**, 2908-2913 (1964).

[3] Faber, V., Joubert, W., Kast, M., Wang, G. M., and Zabel, J., to be submitted to *SIAM J. of Appl. Math.*

CAPTIONS

Figure 1. The physical processes and codes used to model these processes in the virtual prototyping.

Figure 2. LAHET model of energy/angle dependence of gamma-ray production. Each angle bin is 5 degrees.

Figure 3. Reconstruction from MCNP data.

Figure 4. Reconstruction from RATRACE data. A cross-section of 0.03 cm**2/g (non-resonant) was required to match MCNP.

Figure 5. MCNP simulation of a 3" x 3" BGO monitor detector with a multiple gamma-ray source from the composite target.

Figure 6. One slice of a non-resonant reconstruction from computer simulated data. There are 3 small objects of density 1.1 and 3 large objects of density 0.2 each surrounded by 2 small cylindrical shells of density 1.1.

Figure 7. A 16 detector 16 view reconstruction from cobalt 60 data of a cylindrical shell.

Figure 8. A 16 detector 32 view reconstruction from accelerator data of a 5 mm vertical sheet.

Nature of Process	Code Used
proton beam transport	LAHET
proton target interaction	LAHET
gamma ray production	LAHET
energy dependence	
angle dependence	
transport of gamma rays to the detector	MCNP and RATRACE
interaction of gamma rays with detector	MCNP
production of light in the detector	GUIDE7
tomographic reconstruction	CORMACK
image processing and alarm system	KHOROS

LAHET	Los Alamos High Energy Transport
MCNP	Monte Carlo Neutonics Photonics
RATRACE	A ray tracing code to build tomographic data
GUIDE7	A CERN code
CORMACK	A tomographic reconstruction code based on the Cormack algorithm
KHOROS	A public domain image and signal processing code available from the University of New Mexico

Figure 1. The processes and codes used in the virtual prototyping of the explosives detection project.

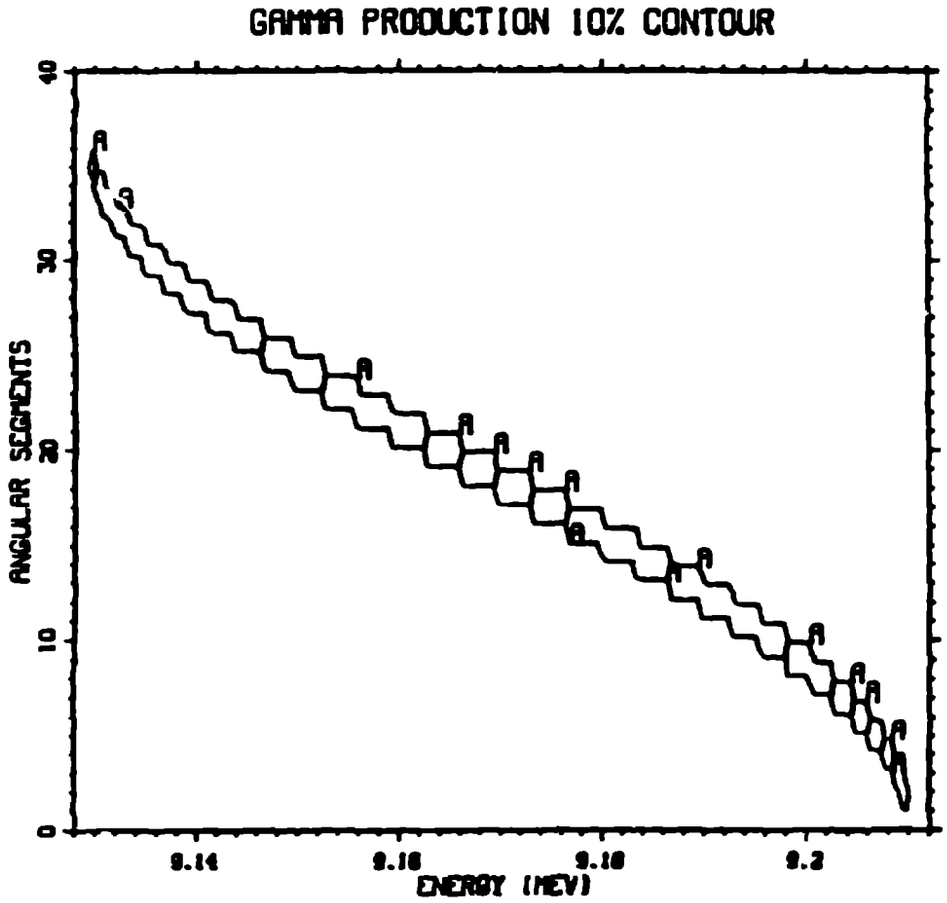
GAMMA PRODUCTION 10% CONTOUR
ANGULAR SEGMENTS
0
10
20
30
40
9.14
9.16
9.18
9.2
ENERGY (MEV)

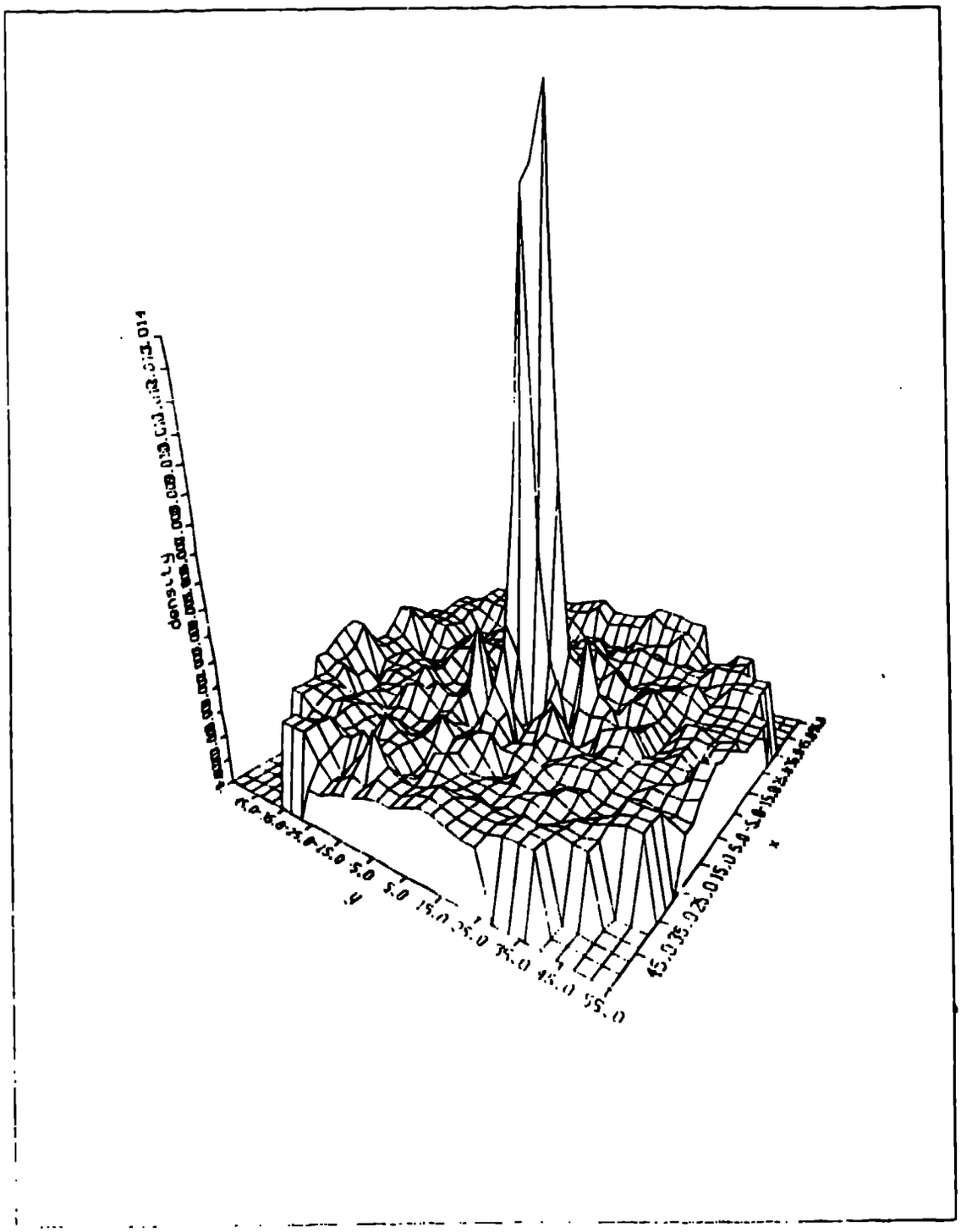

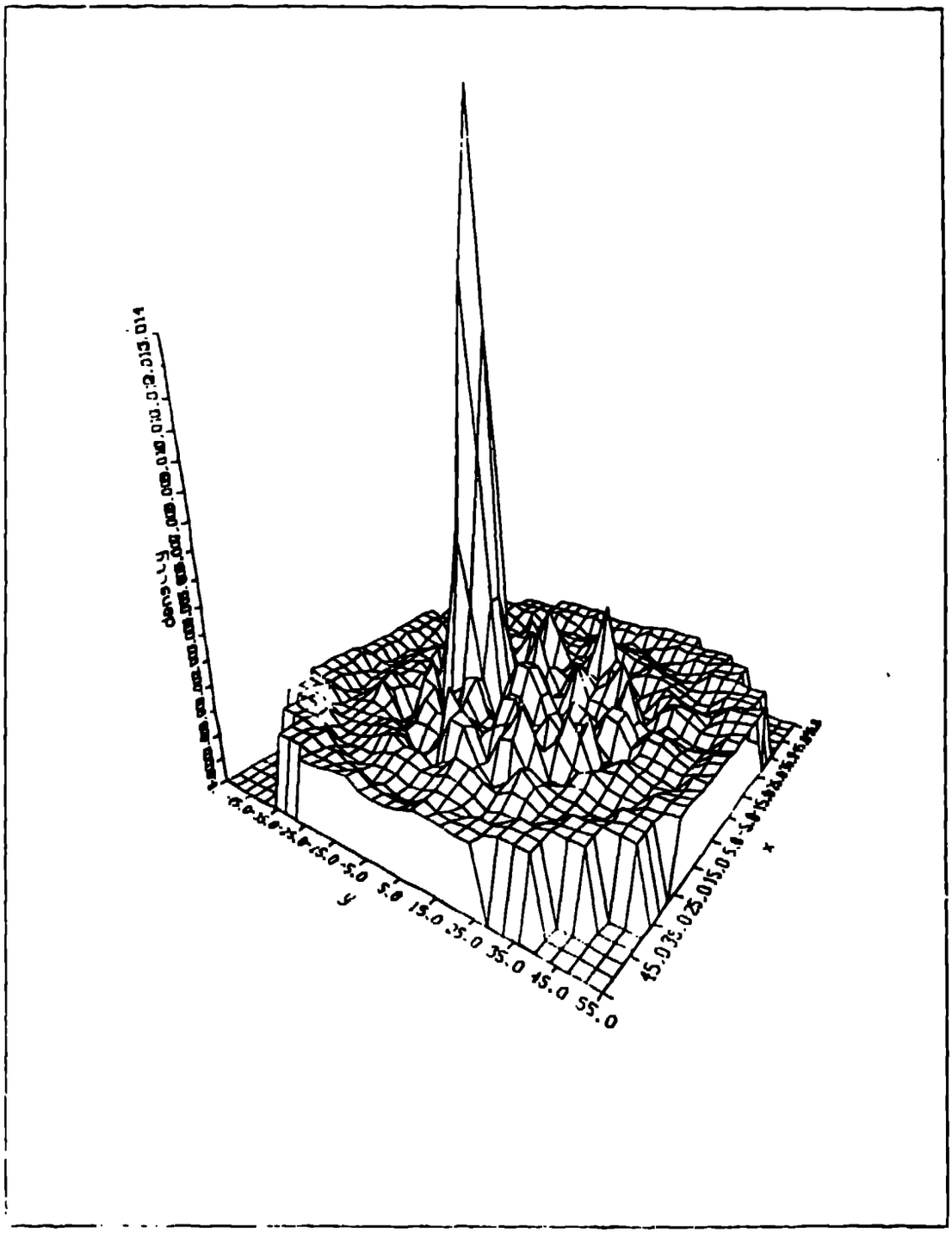
density
y
x
-45.0 -35.0 -25.0 -15.0 -5.0 5.0 15.0 25.0 35.0 45.0 55.0

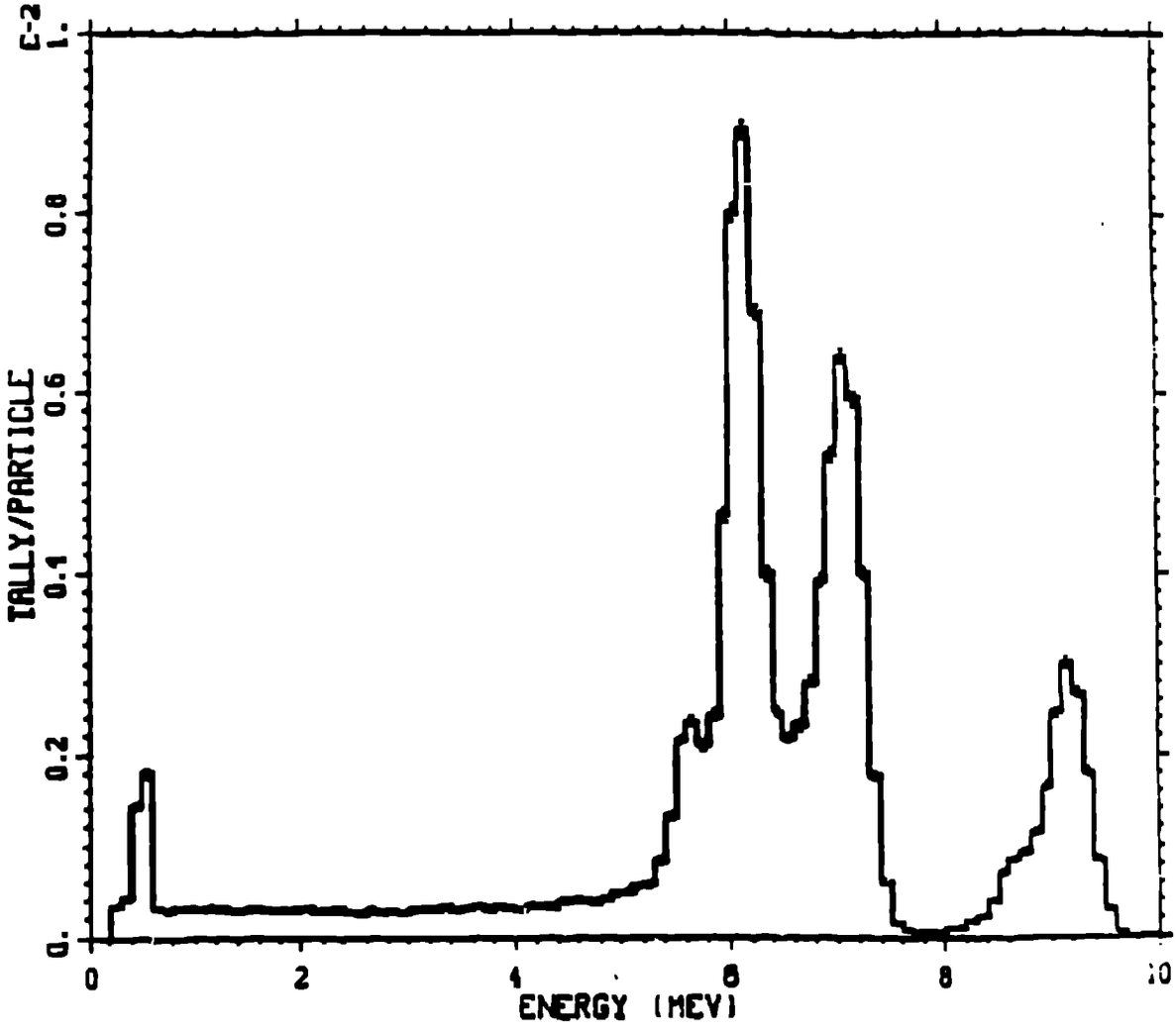

MCNP simulation of the 3" x 3" BGO monitor detector with a multiple gamma-ray source from the composite target.